Journal of Ceramic Processing Research. Vol. 22, No. 1, pp. 79~85 (2021)
(Received 24 July 2020, Received in revised form 2 December 2020, Accepted 4 December 2020)
https://doi.org/10.36410/jcpr.2021.22.1.79

J O U R N A L O F
Ceramic Processing Research

Investigation of urea selective catalytic reduction system with catalyst coated ceramic monolith

Devakaran Karaiellapalayam Palanisamy[a,*] and Arunshankar Jayabalan[b]
[a]*Department of Automobile Engineering, PSG College of Technology, Coimbatore*
[b]*Department of Instrumentation and Control Systems Engineering, PSG College of Technology, Coimbatore*

The selective catalytic reduction (SCR) and fast-SCR retrofit systems effectively control the nitrogen oxides (NO_x) emission for the diesel engine exhaust, using adblue solution and catalyst. The performance characteristic of retrofit system with efficient catalyst and optimum flow channel design, without affecting the engine performance is still a challenging factor. The experimental work is done on a stationary diesel engine test bench coupled to the retrofit system in its exhaust, at steady-state condition. A pair of ceramic monolith coated with cerium oxide (CeO_2) and zeolite (ZSM-5) catalysts are used for pre-oxidation and SCR chambers respectively. The catalysts are characterized by XRD method and dip coated over the ceramic monolith. The static mixer blade inside the middle retrofit pipe is used for homogenization and complete evaporation of adblue solution. The influences of NO_x conversion efficiency of retrofit systems are investigated with the ZSM-5 catalyst and later combined with CeO_2 catalyst. From the experimental results, it is observed that the fast-SCR retrofit system with static mixer blade has a better NO_x conversion efficiency, with marginal decrease in engine brake thermal efficiency than the other retrofit systems at maximum brake power. The increase in brake specific fuel consumption (BSFC) of the retrofit system causes the engine brake thermal efficiency to decrease marginally with increase in brake power.

Keywords: Adblue, Ceramic monolith, CeO_2, Fast-SCR and ZSM-5 .

Abbreviation

NO_x: Nitrogen Oxides
SCR: Selective Catalytic Reduction
PM: Particulate Matter
CeO_2: Cerium Oxide
ZSM-5: Zeolite
LNC: Lean NO_x Catalyst
LNT: Lean NO_x Trap
CRDI: Common Rail Direct Injection
EGR: Exhaust Gas Recirculation
DOC: Diesel Oxidation Catalyst
AOC: Ammonia Oxidation Catalyst
BSFC: Brake Specific Fuel Consumption

Introduction

The major pollutants of the diesel engine exhausts are NO_x and particulate matter (PM) in a lean-burn combustion environment [1, 2]. The development of retrofit technologies such as lean NO_x catalyst (LNC), lean NO_x trap (LNT), common rail direct injection (CRDI) and exhaust gas recirculation (EGR) reduces the NO_x emissions, but the efficiency of diesel engine is affected [3]. The SCR retrofit technology is considered to be effective after treatment method, to regulate the NO_x emissions for stationary and mobile diesel engines [4]. The emerging SCR technology involves a very precise quantity of adblue injected into the upstream of the SCR catalytic chamber [5]. In this process, the reactant ammonia (NH_3) is produced by injecting an adblue through hydrolysis reaction as given in equation (1). The ammonia then reacts with NO_x over the SCR catalyst either as standard SCR reaction or fast-SCR reaction given in equation (2) and equation (3) respectively. The pre-oxidation catalyst promotes the oxidation reaction as given in equation (4) which initiates the fast-SCR reaction.

$$(NH_2)_2CO + H_2O \rightarrow CO_2 + 2NH_3 \quad (1)$$

$$4NH_3 + 4\,NO + O_2 \xrightarrow{\text{Catalyst}} 4N_2 + 6\,H_2O \quad (2)$$

$$4NH_3 + 2\,NO + 2NO_2 \xrightarrow{\text{Catalyst}} 4N_2 + 6H_2O \quad (3)$$

$$2NO + O_2 \xrightarrow{\text{Catalyst}} 2\,NO_2 \quad (4)$$

The incomplete chemical conversion of adblue forms an undesirable salt deposition at the bottom of the retrofit tailpipe which adversely affects the SCR catalyst activity [6]. The excess of adblue injection into the engine exhaust yields NH_3 slip at the tailpipe [7]. The design of adblue injection parameters such as injector nozzle, injection position, injecting temperature

*Corresponding author:
Tel : +91422 4344281
Fax: +91422 2573833
E-mail: kpd.auto@psgtech.ac.in

and injecting quantity also determines the NO_x conversion efficiency [8, 9].

The design of SCR retrofit system for the diesel engine is investigated with diesel oxidation catalyst (DOC), two SCR catalytic chambers and ammonia oxidation catalyst (AOC) and the effects of NO_x reduction efficiency are measured at steady-state condition [10]. An integration of DOC, catalytic diesel particulate filter (CDPF) and SCR retrofit systems are designed and experimented to evaluate the effects on PM and NO_x emissions as per stringent emission norms [11,12].

Research has also focused on the design of novel SCR catalysts such as $V_2O_5/WO_3/TiO_2$, Fe/Cu-zeolite, ZSM-5 and Mn-based catalyst. The operating temperature of $V_2O_5/WO_3/TiO_2$ catalyst is only between 260 ºC to 450 ºC but has difficulty in NH_3 storage [13, 14]. The binary and ternary ($V_2O_5/WO_3/TiO_2$) catalyst samples are examined by structural analyses and later NO_x reduction efficiency is determined at different loadings and various temperature ranges [15]. The Fe-zeolite catalyst is operated up to 600 ºC but prone to stability problems at higher temperature in the presence of moisture [16]. The Cu-zeolite catalyst has higher NO_x conversion efficiency only between 200 ºC to 400 ºC but its durability is inadequate [17]. Mn-based catalyst has better performance but the efficiency is affected by its calcination temperature and O_2 concentration in the reaction medium [18]. The CeO_2 catalyst is a promising material for fast oxygen sensors at high temperature, because of its chemical stability and high diffusion coefficient of oxygen vacancies [19]. The different types of Zeolite with various Si:Al ratio are used as SCR catalyst for NO_x reduction [20].

A ceramic monolith substrate with parallel flow channels of either square or triangular cells coated with catalytic material is extensively used for automotive and stationary SCR control reactors [21]. The internal flow distribution of gases in the retrofit system has a greater effect on NO_x conversion efficiency. To enhance the performance, different types of mixers are designed and investigated for the SCR retrofit system [22]. A novel static mixer blade inside the retrofit system improved the uniform mixing of gases, which has better NO_x conversion efficiency than commercially available mixer blade [23]. An improved NO_x conversion rate is obtained with combination of two static mixer blades as compared with single static mixer blade in the retrofit system [24].

In the literature, optimizing factors such as adblue injection strategy, catalyst loading and static mixer blade are investigated separately at different experimental conditions, for enhancing the NO_x conversion efficiency of diesel engine retrofit system. It is observed that there are still more chances for improving the performance characteristics of the retrofit system, without affecting the engine performance. The main contribution of this experimental work is the improvement in NO_x conversion efficiency of diesel engine retrofit system, with the combined effect of pre-oxidation and SCR catalysts coated over ceramic monolith.

Catalyst Characteristics and Coating Method

Catalyst selection

The cerium oxide (CeO_2) and zeolite (ZSM-5) catalysts are selected for the pre-oxidation and SCR chambers respectively. The catalyst CeO_2 can become non-stoichiometric in oxygen content depending on its ambient partial pressure of oxygen. In association with other catalysts, CeO_2 is economical and promotes oxidation reaction to convert harmful emission to harmless [25]. The diesel engine exhaust contains 90% NO and 10% NO_2 and by usage of CeO_2 as pre-oxidation catalyst, it equalizes the concentration NO_x into 50% NO and 50% NO_2 which enhances the fast-SCR reaction [26].

The ZSM-5 is the most active catalyst at low and high temperatures for ammonia SCR reaction. It provides higher thermal stability to exhaust gas temperature and also has better NO_x conversion efficiency when compared to other catalysts [27].

Catalyst characterization

The standard procedure is adopted for catalyst characterization as given in [28]. The crystallinity and structure of catalysts are analyzed by X-ray diffraction (XRD) technique using Cu Kα radiation (45 kV, 30 mA). The scanning is operated in the 2θ range of 5º to 90º with a scanning speed 4.02 deg/min. The XRD pattern of CeO_2 used for pre-oxidation catalyst is shown in the Fig. 1. The diffraction peaks at 2θ = [28.5, 47.5, 56.3, 69.4, 76.7, 88.7] are observed and these peaks attribute to the cubic structure of CeO_2.

The standard procedure is adopted for SCR catalyst characterization as given in [29, 30]. The XRD pattern of ZSM-5 with Si:Al ratio of 50:1 is shown in the Fig. 2. The diffraction peaks are observed at 2θ = [7.9, 14.7,

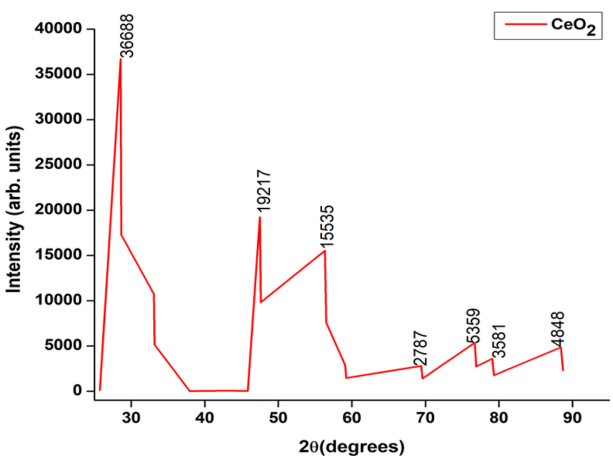

Fig. 1. XRD pattern of CeO_2 catalyst.

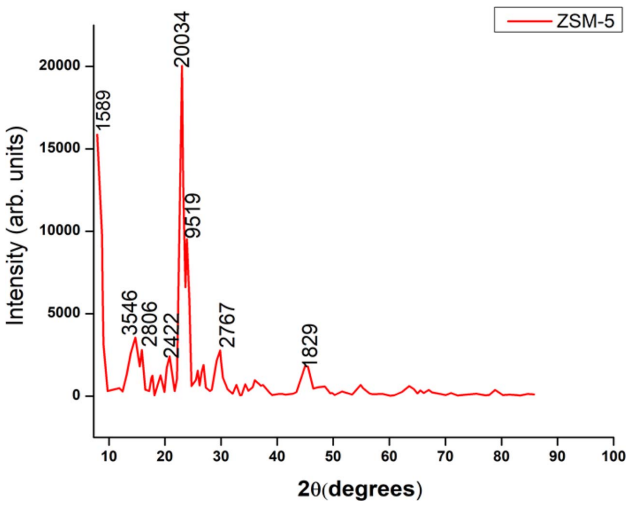

Fig. 2. XRD pattern of ZSM-5 catalyst.

15.8, 20.8, 23.04, 23.8, 24.3, 29.8, 44.9] and these attributes to the combination of decasodium dihydrogendodecatungstate 27-hydrate substructure and tungsten oxide which are anorthic and monoclinic in crystal structure respectively.

Catalyst coating techniques

Washcoat preparation

The standard procedure is followed for wash coating over the ceramic monolith as given in [31, 32]. The first step involves the selection of appropriate volumes of ceramic monolith for pre-oxidation and SCR chambers. Initially, the weight of the ceramic monolith is measured. 100mL of distilled water is added and allowed to stir using a magnetic stirrer. Then 10 gm wt% of Al_2O_3 is added and allowed to stir well for a few minutes. Subsequently, glacial acetic acid (CH_3COOH) is added gradually and stirred well. The above procedure is repeated until pH of 2-3 is obtained, after which the ceramic monolith is dipped into the slurry for a few seconds. After the monolith pore is cleared using a blower and dried in the oven for few minutes and later cooled to room temperature. Finally, the weight gained over ceramic monolith is measured and the above procedure is repeated until the required amount of Al_2O_3 gets coated over the ceramic.

The initial weight of the monolith is 18.1428 gm. The weight gained by the ceramic monolith after tenth immersion is 4.2530 gm. Then the washcoat procedure is repeated for other volume of ceramic monolith.

SCR and pre-oxidation catalyst incorporation

After wash coating, the standard procedure given in [33, 34] is followed during dip coating of ZSM-5 and CeO_2 catalyst for SCR and pre-oxidation chamber respectively. Initially, the ceramic monoliths are dipped inside the respective catalyst solutions and then stirred using an ultrasonic bath. The water is removed by an air blower inside the ceramic monolith. Then the monoliths are placed inside a furnace at 100 °C for about 15 min to dry the water and cooled to room temperature. Finally, the above procedure is repeated until the required amount of catalyst gets coated over the substrate. The weights gained by the monoliths after fifteenth immersion are 5.3459 gm and 4.5824 gm for SCR and pre-oxidation catalyst respectively.

Experimental Setup and Method

Experimental setup

The schematic representation and picture of the engine test bench used for the experimental work are shown in Figs. 3-4. The test bench comprises a stationary diesel engine, with its specifications given in Table 1. The diesel engine is directly coupled to a dynamometer through a propeller shaft with a universal joint for controlling the engine load strategy. The specifications of dynamometer are given in Table 2.

The volume of ceramic monolith depends on the engine displacement volume [35, 36]. A pair of ceramic monoliths are selected and coated with suitable catalyst for pre-oxidation and SCR chamber. The catalyst specifications are given in Table 3. The detailed specifications of the catalytic substrates are given in Table 3. An optimized static mixer blade comprising of eight blades, with the blades inclined at 45° are welded inside the middle retrofit pipe located after the adblue injection. The specifications of adblue associated components are given in Table 4. An exhaust gas analyzer is used to measure the NO_x emission and their specifications are listed in Table 5.

Experimental Method

The engine test bench is started and warmed for 15 minutes. The intake system supplies sufficient air to run the engine. The direct torque control strategy is employed to the dynamometer, with the engine speed fixed at 1,500 rpm. The adblue is injected during the engine exhaust stroke period and a certain temperature of the exhaust gas. The rotary encoder measures the engine crank rotation for estimating period and the thermocouple measures the exhaust gas temperature for initiating adblue injection at 180 °C to 200 °C. The total fuel consumption at engine dynamometer scale and exhaust NO_x emission are measured for no-load condition. Then the dynamometer load is increased to 3 kg which decreases the engine speed. To maintain the engine at constant speed, the total fuel consumption increases and their corresponding NO_x emission is measured. This experimental procedure is repeated by changing the loads at equal intervals from no load to 12 kg in steps of 3 kg which represents 25% increase in engine brake power. The control of adblue injection quantity during the experiment is 50 mg/s. The efficiency of NO_x conversion of retrofit systems, are investigated

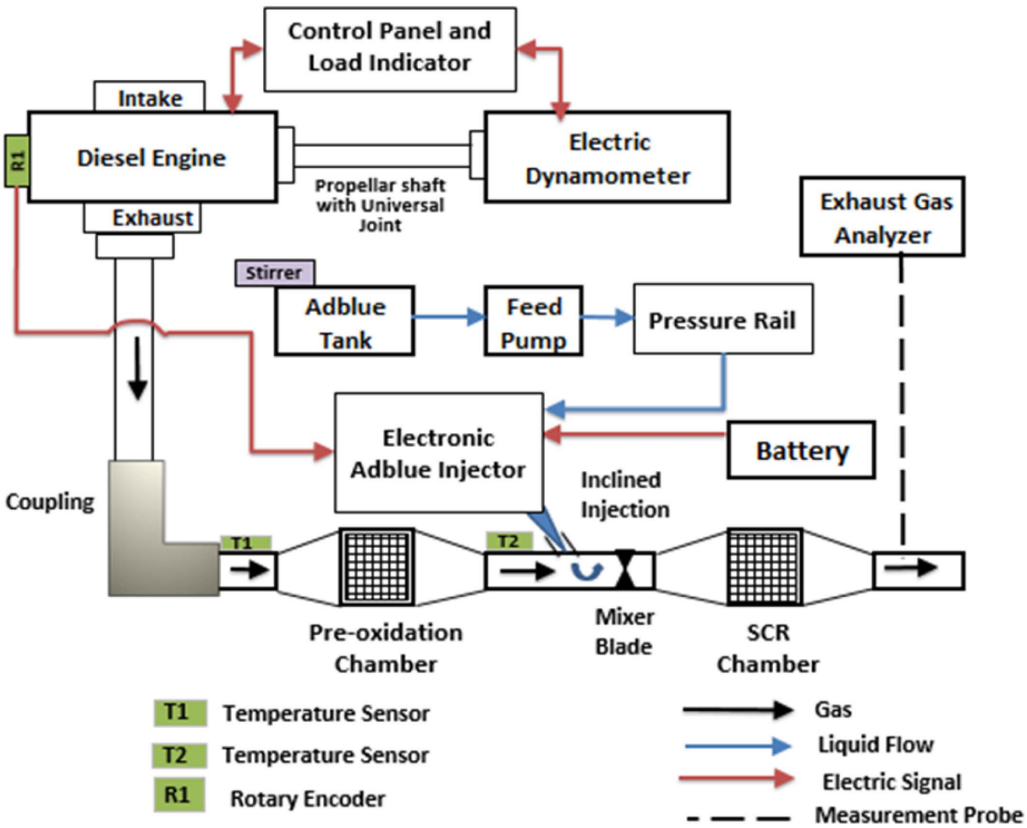

Fig. 3. Schematic of Diesel Engine Test Bench Setup

Fig. 4. Picture of engine test bench setup with retrofit system

Table 1. Specifications of Diesel Engine

Make and Model	Kirloskar and VCR
Engine type	4 stroke, constant speed
Type of fuel	Diesel
Number of cylinders	1
Maximum power	3.5 kW
Cylinder bore X stroke	87.5 X 110 mm
Compression ratio	17.5:1
Swept volume	661 cc
Fuel tank	15 liters

Table 2. Specifications of dynamometer.

Make and Model	Technomech
Dynamometer type	Eddy current, water-cooled
Maximum power	7.5 kW
Speed	1,500 - 4,500 rpm
Load range	0 - 25 kg

Table 3. Technical specifications of catalyst support

Catalytic substrate	Ceramic monolith
Catalytic volume	331 cc
Cell structure	Square
Range of cell density	300 cpsi
Porosity of the cells	0.4575

Table 4. Specifications of Adblue Assisted Components

Adblue tank capacity	12 liters
Adblue feed pump supply voltage and output pressure range	12 V and 3 - 5 bar
Adblue common rail pressure	8 - 10 bar
Adblue injector angle and nozzle injection pressure	50° and 7 bar
Thermocouple sensor range	-50 to 1100 °C
Rotary encoder range	0 to 360° rotation and 60 CPR
Development board and Microcontroller	Arduino Uno-R3 and ATmega 328

Table 5. Technical Specifications of Exhaust Gas Analyzer.

Model	AVL 444
Type	Five gas exhaust analyzer
Parameter studied	NO_x
NO_x range	0 - 5000 ppm vol.
NO_x accuracy	± 50 ppm vol.

with SCR catalyst and later combined with pre-oxidation catalyst, with and without static mixture blade.

Results and Discussion

Effect of brake power on brake thermal efficiency

To study the effect of brake power on brake thermal efficiency, the brake power is increased from zero to full load at equal intervals of 25% as discussed in the experimental method. The results show that the brake thermal efficiency increases, with increase in brake power for the retrofit systems, as given in Fig. 5. The engine operating temperature increases with increase in brake power and hence, the brake thermal efficiency increases.

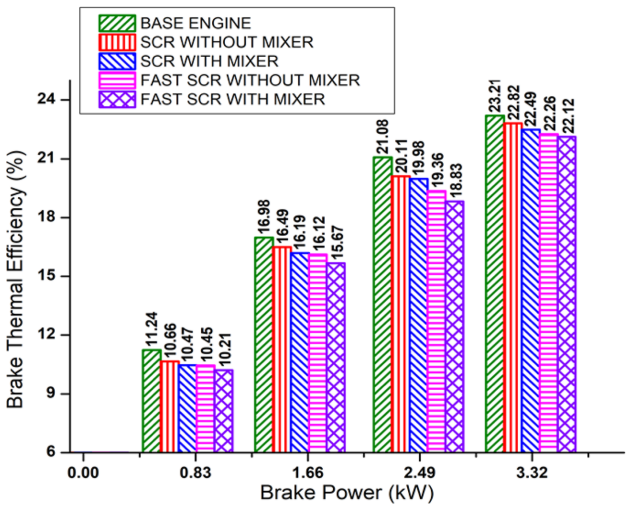

Fig. 5. Effect of brake power on brake thermal efficiency.

The brake thermal efficiency of the base engine is 23.21% at maximum brake power. The presence of catalytic filters restricts the exhaust gas, which reduces the engine brake thermal efficiency for SCR and fast-SCR systems without static mixture blade, by 0.39% and 0.95% respectively at maximum brake power. After the static mixture blade has been fitted inside the middle of the retrofit pipe, the restriction of exhaust gas further increases and hence, the reduction of engine brake thermal efficiency for SCR and fast-SCR retrofit systems improved to 0.72 % and 1.09 % respectively at maximum brake power.

The experimental results show the performance of the diesel engine with respect to brake thermal efficiency decreases marginally after the retrofit systems are coupled to the engine exhaust even at maximum brake power.

Effect of brake power on NO_x reduction

The effects of brake power on NOx reduction for the retrofit systems are shown in Fig. 6. From the results, it is observed that the engine cylinder peak temperature increases, with increase in brake power and hence the NO_x increases.

The NO_x of base engine without the retrofit system is 494 PPM at maximum brake power. When the adblue and the catalyst react with the exhaust gas, NO_x conversion efficiencies are 81% and 86% for SCR and fast-SCR retrofit system without static mixer blade respectively at maximum brake power.

After the static mixer blade is fixed, uniform mixing of adblue solution with exhaust gas occurs and hence,

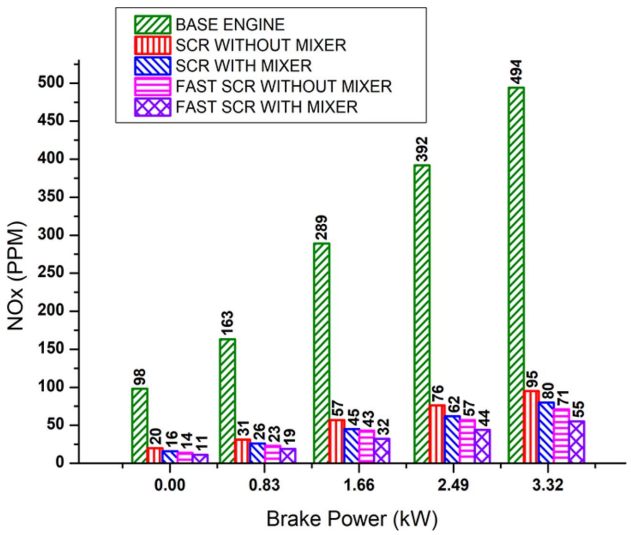

Fig. 6. Effect of brake power on NO_x reduction.

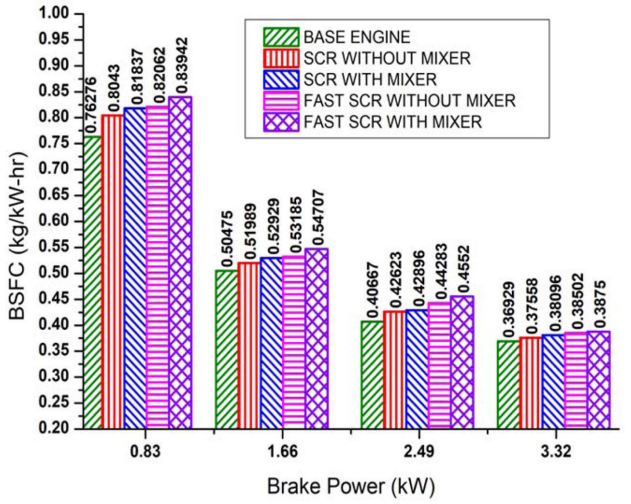

Fig. 7. Effect of brake power on BSFC.

the NO_x conversion efficiency is further improved to 84% and 89% for SCR and fast-SCR retrofit systems respectively at maximum brake power. The highest NO_x conversion efficiency of the retrofit system is due to the combined effect of pre-oxidation and SCR catalyst with mixer blade.

Effect of brake power on brake specific fuel consumption

From the results, it is observed that brake power increases with increase in total consumption of fuel and hence, the BSFC decreases as shown in Fig. 7.

The BSFC of the base engine is 0.369 (kg/kW-hr) at maximum brake power. The presence of catalytic filters restricts the exhaust gas, which increases the BSFC for SCR and fast-SCR systems without static mixture blade, to 0.375 (kg/kW-hr) and 0.385 (kg/kW-hr) respectively at maximum brake power. After, the static mixture blade is fixed inside the retrofit pipe the restriction of exhaust gas further increases and hence, the BSFC for SCR and fast-SCR retrofit systems are further increased to 0.380 (kg/kW-hr) and 0.387 (kg/kW-hr) respectively at maximum brake power. The increase in BSFC causes the brake thermal efficiency of the engine to decrease with increase in brake power.

Conclusion

In this work, control of NO_x emission for the retrofit system and the performance of diesel are investigated. The retrofit system with SCR catalyst and then combined with pre-oxidation catalyst, with and without static mixture blade are examined. From the experimental results, the relative NO_x conversion efficiency and reduction in engine brake thermal efficiency are improved for fast-SCR than the SCR retrofit system. The CeO_2 catalyst inside the pre-oxidation chamber promotes the oxidation reaction and enhances NO_x conversion rate with SCR catalyst. The static mixer blade inside the middle retrofit pipe improves the complete evaporation of adblue solution to react with SCR catalyst. The increase in BSFC of the retrofit system causes the engine brake thermal efficiency to decrease marginally with increase in brake power. The highest NO_x conversion efficiency is obtained for fast-SCR retrofit system with static mixer blade, along with marginal decrease in engine brake thermal efficiency, as compared to other retrofit systems at maximum brake power.

References

1. B. Guan, R. Zhan, H. Lin, and Z. Huang, Appl. Therm. Eng. 66[1-2] (2014) 395-414.
2. X. Yuan, H. Liu, and Y. Gao, Emiss. Control Sci. Technol. 1[2] (2015) 121-133.
3. V. Praveena and M.L.J. Martin, J. Energy Inst. 91[5] (2017) 704-720.
4. M. Koebel, M. Elsener, and M. Kleemann, Catal. Today 59[3-4] (2000) 335-345.
5. H.T. Xu, Z.Q. Luo, N. Wang, Z.G. Qu, J. Chen, and L. An, Appl. Therm. Eng. 147 (2019) 198-204.
6. S. Sadashiva Prabhu, N.S. Nayak, N. Kapilan, and V. Hindasageri, Appl. Therm.Eng. 111 (2017) 1211-1231.
7. G. Liu, G.W. Bao, W. Zhang, D. Shen, Q. Wang, C. Li, and K. Luo, J. Energy Inst. 92[5] (2019) 1262-1269.
8. T.J. Wang, S.W. Baek, S.Y. Lee, D.H. Kang, and G.K. Yeo, AIChE J. 55[12] (2009) 3267-3276.
9. K. Bashirnezhad, M. Mehregan, and S.A. Kebriyaee, J. Energy Inst. 89[1] (2016) 115-120.
10. S. Bai, J. Han, M. Liu, S. Qin, G. Wang, and G. Li, Appl. Therm. Eng. 142 (2018) 421-432.
11. A. Ko, Y. Woo, J. Jang, Y. Jung, Y. Pyo, H. Jo, O. Lim, and Y.J. Lee, J. Ind. Eng. Chem. 80 (2019) 160-170.
12. Y. Zhang, D. Lou, P. Tan, and Z. Hu, Atmos. Environ. 177 (2018) 45-53.
13. C.P. Cho, Y.D. Pyo, J.Y. Jang, G.C. Kim, and Y.J. Shin, Appl. Therm. Eng. 110 (2017) 18-24.
14. B.P. Ayo, R.L. Fonseca, and J.R.G. Velasco, Appl. Catal.

363[1-2] (2009) 73-80.
15. B.W. Lee, H. Cho, and D.W. Shin, J. Ceram. Process. Res. 8[3] (2007) 203-207.
16. Y. Shin, Y. Jung, C.P. Cho, Y.D. Pyo, J. Jang, G. Kim, and T.M. Kim, Chem. Eng. J. 381 (2020) 122751.
17. J. Ochonska, D. McClymont, P.J. Jodlowski, A. Knapik, B. Gil, W. Makowski, W. Lasocha, A. Kolodziej, S.T. Kolaczkowski, and J. Lojewskaa, Catal. Today 191[1] (2012) 6-11.
18. J. Tan, Y. Wei, Y. Sun, J. Liu, Z. Zhao, W. Song, J. Li, and X. Zhang, J. Ind. Eng. Chem. 63 (2018) 84-94.
19. G. Balakrishnana, C.M. Raghavan, C. Ghosh, R. Divakar, E. Mohandas, J.I. Songa, S.I. Baea, and T.G. Kim, Ceram. Int. 39[7] (2013) 8327-8333.
20. K. Kamasamudram, N.W. Currier, X. Chen, and A. Yezerets, Catal. Today. 151[3-4] (2010) 212-222.
21. J.L. Williams, Catal. Today. 69[1-4] (2001) 3-9.
22. C. Zhang, C. Sun, M. Wu, and K. Lu, J. Fuel. 237 (2019) 465-474.
23. Q. Wang, D. Zhang, J. Wang, and S. Li, Appl. Mech. Mater. 316-317 (2013) 1156-1161.
24. Y.S. Cho, S.W. Lee, W.C. ChoiI, and Y.B. Yoon, Int. J. of Automotive Technol. 15[5] (2014) 723-731.
25. J.S. Park, J.G. Yeo, S.C. Yang, and C.H. Cho, J. Ceram. Process. Res. 19[1] (2018) 20-24.
26. B.K. Yun and M.Y. Kim, Appl. Therm. Eng. 50[1] (2013) 152-158.
27. J. Shao, S. Cheng, Z. Li, and B. Huang, Catal. 10[3] (2020) 311.
28. Y. Liu, C. Song, G. Lv, C. Fan, and X. Li, Catal. 8[8] (2018) 306.
29. B. Ganemi, E. Bjornbom, B. Demirel, and J. Paul, Microporous and Mesoporous Mater. 38[2-3] (2000) 287-300.
30. Z. Liao, K. Zha, W. Sun, Z. Huang, H. Xu, and W. Shen, Catal. 10[12] (2020) 1377.
31. S.-S. Park, D.-H. Yoon, S.-H. You, W.-T. Bae, and D.-W. Shin, J. Ceram. Process. Res. 9[6] (2008) 591-595.
32. E. Srinivasa Rao and P. Manohar, J. Ceram. Process. Res. 17[5] (2016) 448-453.
33. R. Durairaj, N. Subramanyan, and D. Duraiswamy J. Ceram. Process. res. 20[6] (2019) 621-631.
34. B. Shin, T.W. Dung, and H. Lee, J. Ceram. Process. res. 15[2] (2014) 125-129.
35. B.P. Pundir, in "Engine Emissions: Fundamentals and Advances in Control" (Alpha Science International Ltd, 2017) p.141.
36. V. Ganesan, in "Internal Combustion Engines" (McGraw-Hill Education, 4th Edition, 2015) p.517.